APL MATERIALS **2**, 081513 (2014)

Charge carrier recombination channels in the low-temperature phase of organic-inorganic lead halide perovskite thin films

Christian Wehrenfennig, Mingzhen Liu, Henry J. Snaith,
Michael B. Johnston, and Laura M. Herz[a]
Department of Physics, University of Oxford, Clarendon Laboratory, Oxford OX1 3PU, United Kingdom

(Received 22 May 2014; accepted 18 July 2014; published online 6 August 2014)

The optoelectronic properties of the mixed hybrid lead halide perovskite $CH_3NH_3PbI_{3-x}Cl_x$ have been subject to numerous recent studies related to its extraordinary capabilities as an absorber material in thin film solar cells. While the greatest part of the current research concentrates on the behavior of the perovskite at room temperature, the observed influence of phonon-coupling and excitonic effects on charge carrier dynamics suggests that low-temperature phenomena can give valuable additional insights into the underlying physics. Here, we present a temperature-dependent study of optical absorption and photoluminescence (PL) emission of vapor-deposited $CH_3NH_3PbI_{3-x}Cl_x$ exploring the nature of recombination channels in the room- and the low-temperature phase of the material. On cooling, we identify an up-shift of the absorption onset by about 0.1 eV at about 100 K, which is likely to correspond to the known tetragonal-to-orthorhombic transition of the pure halide $CH_3NH_3PbI_3$. With further decreasing temperature, a second PL emission peak emerges in addition to the peak from the room-temperature phase. The transition on heating is found to occur at about 140 K, i.e., revealing significant hysteresis in the system. While PL decay lifetimes are found to be independent of temperature above the transition, significantly accelerated recombination is observed in the low-temperature phase. Our data suggest that small inclusions of domains adopting the room-temperature phase are responsible for this behavior rather than a spontaneous increase in the intrinsic rate constants. These observations show that even sparse lower-energy sites can have a strong impact on material performance, acting as charge recombination centres that may detrimentally affect photovoltaic performance but that may also prove useful for optoelectronic applications such as lasing by enhancing population inversion. [http://dx.doi.org/10.1063/1.4891595]

Optoelectronic processes in the organic-inorganic perovskites $CH_3NH_3PbI_3$ and $CH_3NH_3PbI_{3-x}Cl_x$ are currently receiving a great deal of attention relating to their successful application in the absorber layer of low-cost solar cells.[1–3] During the past two years, numerous studies have been published on material properties directly related to device performance, such as carrier mobilties,[4–6] recombination lifetimes,[7–9,5,6] excitonic properties,[10,11] and optical absorption.[12–14] Good progress has been made in revealing what enables hybrid lead halide perovskites to deliver such impressive power conversion efficiencies in solar cells.

In order to substantiate the understanding of the underlying photophysics, studies with a scope beyond the conditions defined by a particular application can provide essential further contributions and help verify theoretical predictions from structural and band-structural calculations, which

[a]Author to whom correspondence should be addressed. Electronic mail: l.herz@physics.ox.ac.uk.

have recently been undertaken by several groups.[15–21] Valuable insights can often be gained by isolating the influence of thermal excitation and broadening mechanisms in the system through temperature-dependent studies. Given that reported exciton binding energies in $CH_3NH_3PbI_3$ and $CH_3NH_3PbI_{3-x}Cl_x$ are close to the characteristic thermal energy at room temperature ($k_BT \approx 25$ meV),[10,11,22] low-temperature measurements may shed more light on the role of excitonic states in carrier recombination processes. Furthermore, we have recently shown that phonon-interactions have a significant impact on the luminescence and charge transport properties of these perovskites.[12,41]

To date the results of several temperature-dependent studies on bulk $CH_3NH_3PbI_3$ have been published, which provide important information on structural phase transitions in the material. At temperatures above ~330 K, the compound adopts the simple cubic perovskite structure (space group $Pm\bar{3}m$),[23] although a very small ferroelectric-type displacement of the lead-cation has been observed,[4] which – strictly speaking – creates a tetragonal unit cell (space group P4mm). The transition to the room-temperature phase involves a collective rotation of the PbI_6-octahedra around the c-axis,[24,25] which is well-known from many inorganic perovskites and which leads to closer packing within the *ab*-plane. The resulting unit cell is tetragonal with space group I4cm and has doubled in volume with respect to the cubic unit cell.[24,25] A further transition to an orthorhombic phase is observed at ~160 K.[24,26] This transition is accompanied by a tilting of the PbI_6-octahedra out of the ab-plane and a corresponding further doubling of the unit cell volume (space group Pnma).[26] An analysis of the symmetries of the tetragonal and the orthorhombic phases shows that a continuous transition between the two space groups is not possible. Therefore, a transient intermediate phase has been postulated, but not yet been resolved.[26] The behavior of the "A-cation" $CH_3NH_3^+$, which, other than in purely inorganic perovskites, possesses several rotational degrees of freedom in the high-temperature phase, has been investigated by means of NMR- spectroscopy[27] as well as IR-vibrational spectroscopy,[28] calorimetry,[28] and dielectric measurements.[24,29] It was found that the cubic symmetry of the high-temperature phase is effectively preserved through rapid random reorientations of the $CH_3NH_3^+$-cation. From its 24 possible orientations, 8 remain in the tetragonal phase. Eventually, in the orthorhombic phase, all degrees of freedom are frozen.[27,28]

Information on optical and electronic properties of $CH_3NH_3PbI_3$ at low temperature is very scarce. Apart from the aforementioned dielectric studies reflecting the behavior of the $CH_3NH_3^+$-cation, some data are available on resistivity showing a decrease with increasing temperature as is typical for undoped semiconductors.[4] Very recently, D'Innocenzo *et al.* conducted a study of the excitonic properties of the mixed halide perovskite $CH_3NH_3PbI_{3-x}Cl_x$ for which temperature-dependent optical absorption data have been acquired.[11] The focus of the report however mainly lies on the behavior of the material within the tetragonal (room-temperature) phase. photoluminescence (PL) and diffuse reflectance spectra at low-temperature were also recently acquired by Yamada *et al.* on the pure triiodide $CH_3NH_3PbI_3$ as infiltrated into mesoporous TiO_2.[30]

In this paper, we present a study of the optical absorption and luminescence properties of $CH_3NH_3PbI_{3-x}Cl_x$, scrutinizing the temperature-dependent evolution of recombination pathways in this system. Compact films of about 330 nm thickness were prepared by dual-source evaporation on glass as described in detail in Ref. 12. The same vapor-deposition process was used as for the fabrication of the active layer of high-efficiency planar heterojunction solar cells reported in Ref. 31. Photoluminescence measurements were performed on an experimental setup based on a tuneable Ti:Sapphire laser previously described in Ref. 12. Spectrally resolved detection with a resolution of $\Delta\lambda \leq 2$ nm was accomplished by a combination of grating monochromator and liquid-N_2-cooled Si-CCD-detector. For time-resolved PL measurements by means of time-correlated single photon counting, a fast avalanche-photodiode (time resolution: ~35 ps) was employed. Samples were mounted in a liquid-helium cryostat (Oxford Instruments Microstat), where they remain under vacuum ($p < 10^{-5}$ mbar). Optical absorption spectra were acquired in the same experimental setup through the same collection optics as the PL spectra. A 100 W incandescent lamp was used as a light source.

We first discuss the optical absorption spectra acquired across the temperature range from 4.2 K to 297 K. It has been shown previously that a shift of the absorption edge in energy at about 140 K can be identified in films of $CH_3NH_3PbI_{3-x}Cl_x$ (and at about 170 K in $CH_3NH_3PbI_3$).[11]

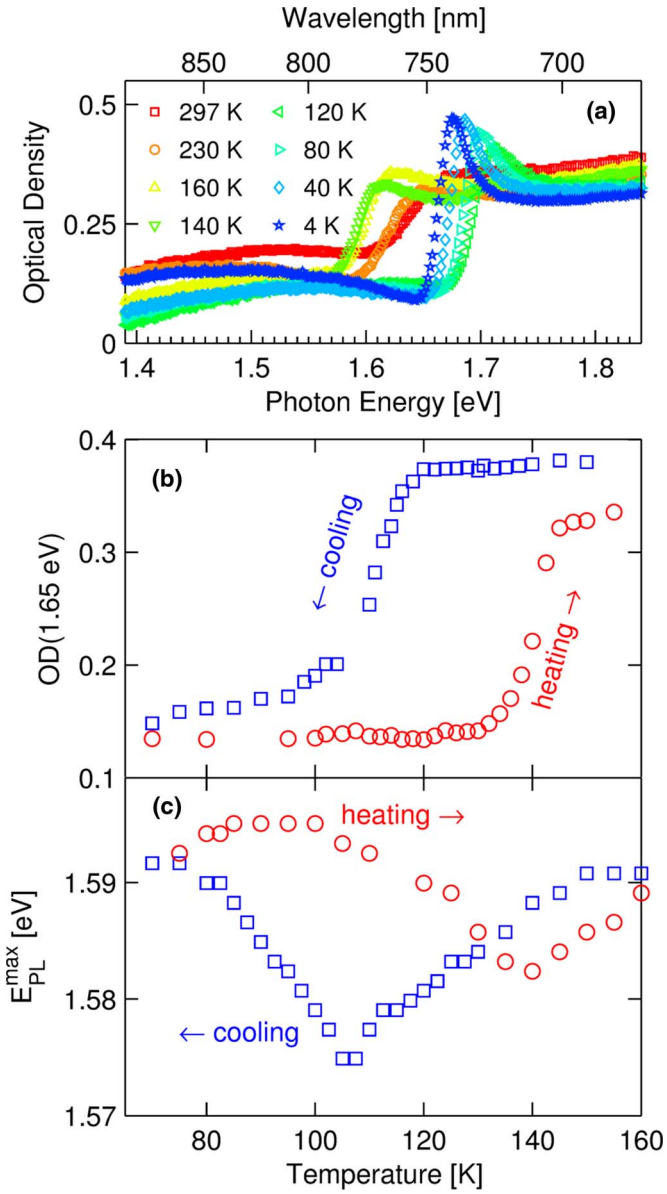

FIG. 1. (a) Optical absorbance spectra of $CH_3NH_3PbI_{3-x}Cl_x$ recorded at temperatures between 4 K and 297 K (heating). (b) Optical density at 1.65 eV photon energy recorded while cooling the sample from 160 K to 40 K (blue squares) at -6 K min^{-1} and while subsequently heating the sample from 40 K to 160 K at 6 K min^{-1} (red circles). (c) Photon energy of maximum PL emission vs temperature (ignoring the higher-energy peak emerging in the low-temperature phase) at excitation fluence 50 nJ cm^{-2} during an identical cooling and heating cycle as in (b).

This shift very likely reflects the same orthorhombic-to-tetragonal phase transition as occurs in the pure halide perovskite $CH_3NH_3PbI_3$, for which an increase in bandgap energy has also been predicted computationally.[26] The optical absorption data recorded in this study are displayed in Fig. 1(a). They show the expected leap of the onset from ~1.7 eV to 1.6 eV between 120 K and 140 K, superimposed on a continuous shift towards higher energy with increasing temperature. The latter represents an unusual behavior of the perovskite when compared to most direct semiconductors, which was recently reproduced in band-structure calculations.[19] At low temperature, the absorption edge is relatively steep and exhibits an overshoot-feature which is most probably to be attributed to resonant formation of excitons.[32] This feature becomes less pronounced towards high temperature along with a continuous broadening of the absorption onset.

In order to locate the orthorhombic-to-tetragonal phase transition more precisely, we scan the temperature range around 140 K with higher resolution. As shown in Fig. 1(b), where the optical density at 1.65 eV is plotted against temperature as an indicator of the completeness of the phase transition, we find strong hysteretic behavior with an about 40 K lower transition when cooling as compared to when heating the sample. We note that even stronger hysteresis is observed when performing an even slower cooling- and heating-cycle (not shown). Previous studies have not come to unique results on this point. While dielectric measurements of $CH_3NH_3PbI_3$ crystals only reveal a hysteresis of a few kelvin,[29] resistivity measurements – also on crystals – exhibit a span of about 30 K between the corresponding features in the heating and the cooling cycle.[4]

We proceed by analyzing PL emission recorded in identical cooling- and heating cycles as performed for optical absorption measurements. Fig. 2 shows a series of temperature-dependent PL spectra at two different excitation fluences. We have discussed the features of room-temperature emission in a recent paper. There, we attributed the relatively large spectral width and the structure of the peak to a homogenous broadening mechanism arising from phonon coupling effects.[12] Within the tetragonal phase, the shape of the peak remains essentially unchanged between 140 K and 297 K, however the overall spectral width decreases with temperature consistent with a smaller available phonon population. The shape of the PL emission is also found to be independent of excitation fluence in this phase ruling out contributions of defect broadening. Such contributions would be expected to show either saturation effects or decrease in their relative strength when entering the regime of bi-molecular recombination processes at stronger excitation.

Interestingly, at temperatures below the phase transition and under high-fluence excitation, we continue to observe emission centred around the same energy as in the room-temperature phase. This is surprising given the increase in bandgap energy by 0.1 eV seen in the optical absorption data. In Fig. 1(c), we inspect the transition regime more closely by plotting the position of the emission maximum against temperature. We identify a feature consisting in a sharp reversal of the continuous drift of the PL peak. For both, the heating and the cooling cycle, this feature coincides with the spontaneous shift of the absorption edge (Fig. 1(b)). The fact that no spontaneous shift of the PL peak is observed, suggest that emission still originates from the same intraband transition on both sides of the structural phase transition. Towards lower temperatures, a second, small, higher-energy emission peak appears gradually, which is located close to the corresponding absorption onset. Note that the spectral width of this peak does not decrease with temperature and substantial broadening is still effective even at 4 K. This observation is consistent with the polaronic mechanism suggested for the homogenous spectral broadening at room temperature, which has been shown to characteristically lead to a remaining finite line width, even at very low temperatures.[33,34] Overall, the PL emission spectrum becomes strongly dependent on excitation fluence below the phase transition. While at low excitation fluence the higher-energy peak almost disappears, the lower-energy peak significantly broadens and drops to even lower energy.

As an explanation for the observed emission behaviour in the low-temperature phase, we consider the possibility of small inclusions of crystallites adopting the room-temperature tetragonal phase. Coexisting crystallographic phases have been observed in several inorganic perovskite materials of mixed[35–37] and pure[38–40] composition. For the latter case, it has been shown that the secondary phase can be stabilized through the effect of strain imposed on a thin film by the substrate[38,39] or through external pressure.[40] Despite the fact that $CH_3NH_3PbI_{3-x}Cl_x$-films studied here were grown on an amorphous glass substrate, and hence any lattice-mismatch of the as-grown sample is ruled out, unequal thermal expansion and, more importantly, the spontaneous change of the in-plane lattice constants during the phase-transition[26] may well cause a significant amount of strain to the film.

Tetragonal inclusions in the orthorhombic phase of $CH_3NH_3PbI_{3-x}Cl_x$ can potentially trap photoexcited carriers due a possibly lower-lying conduction band in this phase (as suggested by the 0.1 eV lower gap). Thus, a large density of carriers would agglomerate and eventually recombine within these inclusions. This scenario straightforwardly rationalizes the fluence-dependent emission spectra. Under strong excitation, the carrier density in tetragonal crystallites saturates, such that a significant number of carriers remains in the orthorhombic phase, hence causing substantial emission at the correspondingly higher energy. In contrast, under weak excitation, the low number of initially free carriers can just partially fill the sub-gap distribution of states in the tetragonal crystallites. A

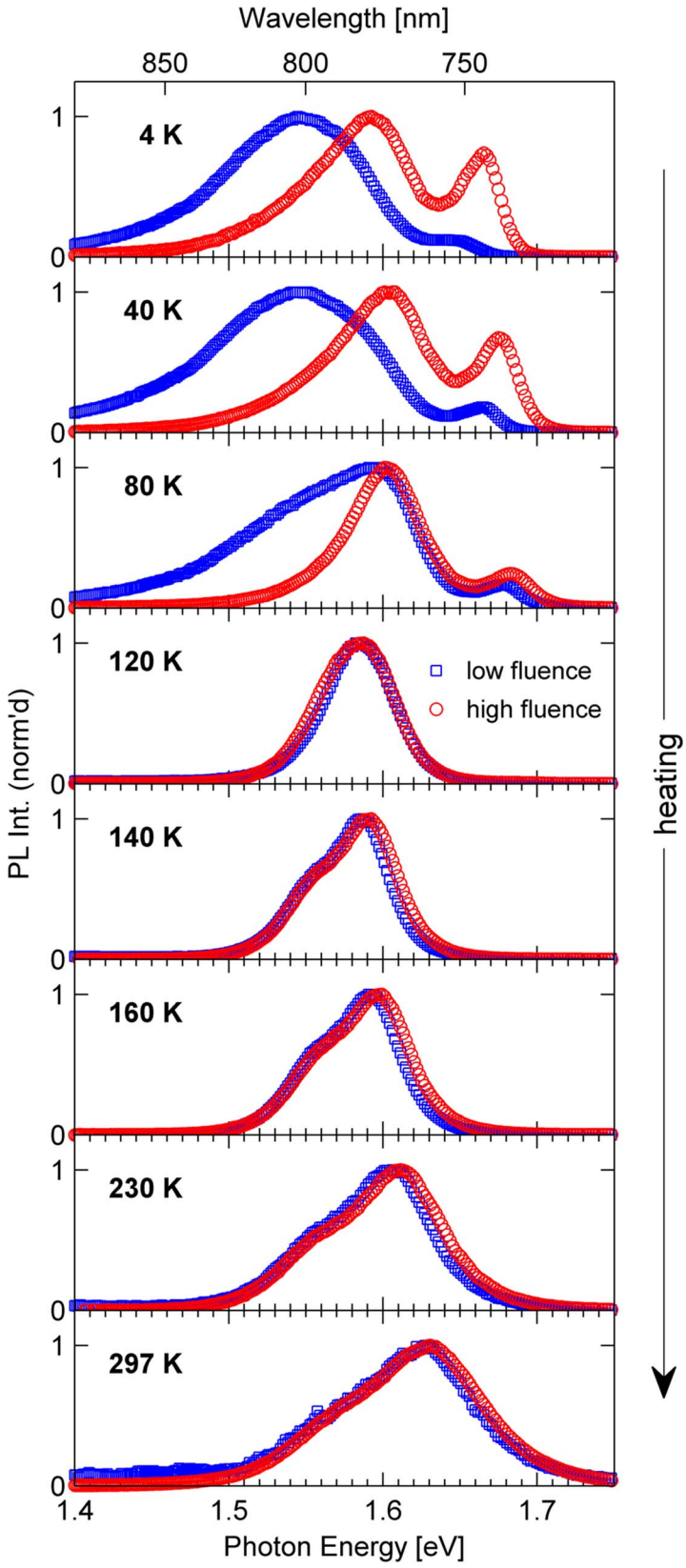

FIG. 2. Photoluminescence spectra of $CH_3NH_3PbI_{3-x}Cl_x$ at temperatures between 4 K and 297 K taken at excitation fluences 5 μJ cm^{-2} and 50 nJ cm^{-2}. Spectra were taken in a single temperature sweep from 4 K to 297 K.

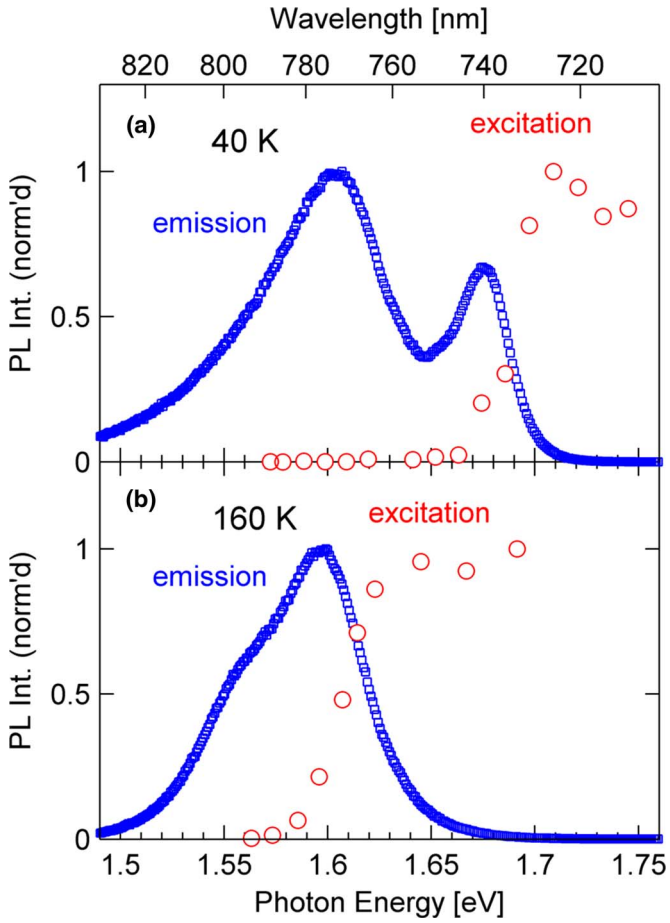

FIG. 3. Normalized photoluminescence excitation spectra (red circles), i.e., spectrally integrated PL emission as a function of excitation energy, at (a) 40 K and (b) 160 K, recorded under continuous wave excitation at an intensity of 5 W cm^{-2}. To provide sensible reference points, normalized PL emission spectra as displayed in Fig. 1 (fluence 5 μJ cm^{-2}) are added to the plot (blue circles).

high density of sub-gap states located at the phase boundaries is plausible, if individual crystallites are assumed to be very small. As a consequence, a broadened and downshifted emission is observed from these carriers.

In order to verify the proposed physical mechanism for the emission characteristics in the low-temperature phase of the $CH_3NH_3PbI_{3-x}Cl_x$ film, we record excitation-energy dependent PL spectra. In Fig. 3(a), the spectrally integrated emission is plotted against excitation energy at 40 K. From comparison of emission and excitation spectrum it becomes clear that, although the strongest emission is observed at about 1.6 eV, i.e., corresponding to the bandgap of the tetragonal phase, measurable excitation through this transition does not appear to be possible. In fact photoexcitation seems to occur exclusively through the higher-energy transition at ~1.7 eV corresponding to the bandgap of the orthorhombic phase. This suggests that the relative volume fraction of low-energy sites is very small, while at the same time, these sites provide the dominant radiative recombination route.

Further insight into the recombination pathways in the orthorhombic and tetragonal phases of $CH_3NH_3PbI_{3-x}Cl_x$ films can be gained from studying their dynamics through time-resolved PL measurements. We have recorded PL decay traces by means of time-correlated single photon counting below and above the phase transition. Fig. 4(a) shows time-dependent PL at 40 K under two different excitation fluences at the maxima of both emission peaks. First, we observe that decay lifetimes as compared between the two emission energies (1.61 eV and 1.69 eV) at the same

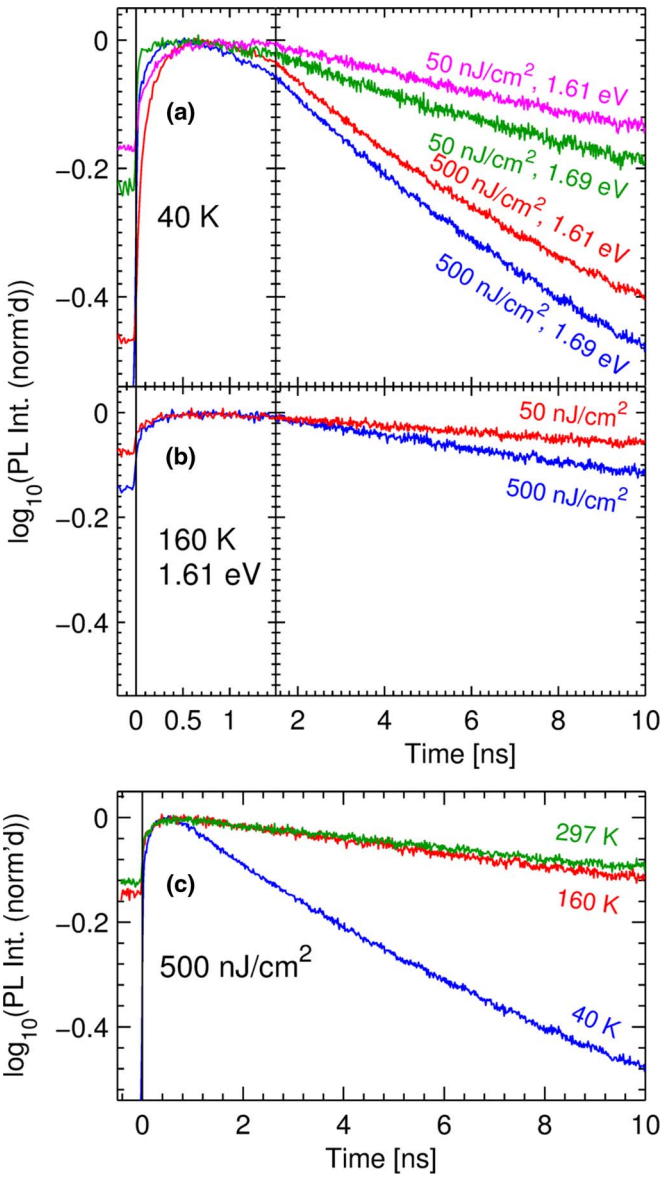

FIG. 4. Time-resolve photoluminescence emission recorded by means of time-correlated single photon counting at various temperatures, excitation fluences and emission energies: (a) T = 40 K. Traces were recorded at both spectral emission maxima. Labels on curves show excitation fluence and detected energy. (b) T = 160 K. Traces were recorded at the spectral emission maximum. Labels on curves show the excitation fluence. (c) Comparison of time-resolved PL at 4 K, 160 K, and 297 K at excitation fluence 500 nJ cm^{-2}. Traces were recorded at the (higher energy) spectral emission maximum. Excitation energy in all panels: 2.43 eV.

excitation fluence are very similar. Focussing on the signal rise it can furthermore be seen that the low-energy emission builds up with about 1 ns delay with respect to the emission at higher-energy. These observations support the proposed scenario of excited carriers largely transferring to low-energy sites (i.e., small tetragonal crystallites) before recombining there. As a consequence of the charge carrier migration being much faster than their recombination, the decay of both populations, in the orthorhombic host-phase and the tetragonal inclusions, is predominantly governed by the (faster) recombination process within the inclusions.

We find that the decay lifetime of photoexcited carriers in the $CH_3NH_3PbI_{3-x}Cl_x$-film depends significantly on excitation fluence, with the decay becoming faster for higher carrier density. This

is a signature of a bi-molecular recombination component.[5] In contrast, only a negligible excitation fluence dependence of the PL decay is observed above the phase transition (see Fig. 4(b)). The latter agrees well with room temperature studies, which show that within the range of excitation densities used ($\sim 5 \times 10^{15}$ cm^{-3} for 50 nJ cm^{-2}), carrier decay is dominantly governed by mono-molecular processes, since the bi-molecular rate constant is very small in the material.[5,41] This does however not imply that the tetragonal-to-orthorhombic phase transition involves a dramatic increase of the bi-molecular rate constant, since it can already be accounted for by the assumed carrier migration to small tetragonal phase inclusions. Because the effective carrier density within these would be much higher than in a homogenous distribution upon photoexcitation, a substantial rise of bi-molecular contributions is expected even if the intrinsic rate constant does not change. This observation also explains the overall faster carrier decay in the low-temperature phase indicated by Fig. 4(c), which directly compares PL transients at 40, 160, and 297 K.

The findings of this study further our understanding of how structural phase transitions in thin films of hybrid metal halide perovskites influence their film morphology and in turn their optoelectronic properties. For photovoltaic applications, the role of inclusions of lower bandgap is likely to be predominantly detrimental, trapping charges and enhancing recombination. It is particularly interesting that the tetragonal phase present at room temperature appears to be free of such inclusions despite the fact that a further phase transition is expected near ~330 K, above which $CH_3NH_3PbI_3$ adopts the simple cubic perovskite structure.[23] Whether cubic inclusions are absent in the room temperature structure of $CH_3NH_3PbI_{3-x}Cl_x$ films, or whether they may be present but relatively ineffective as charge-carrier recombination centres will require further investigations. However, our results show that inclusions of material with different crystal structure can strongly affect these materials even for a very small volume fraction of such inhomogeneities, presumably because of the large charge-carrier diffusion lengths observed for the room temperature phase of $CH_3NH_3PbI_{3-x}Cl_x$.[5,41] We note that similar effects may potentially be present in hybrid metal-halide perovskites that can exhibit compositional variations, such as the formamidinium-based system $FAPbI_yBr_{3-y}$, for which lattice instabilities and dual photoluminescence emission has been observed for values of $y \approx 0.6$–0.8.[14]

For optoelectronic applications, on the other hand, the presence of inclusions with lower potential energy may provide efficient fluorescence centres. Hybrid metal-halide perovskites have recently been suggested as active materials for lasing applications.[12,42,43] Here, lower-energy inclusions may act as recombination centres with locally enhanced population inversions that lower thresholds for lasing, in analogy to low-dimensional semiconductor designs that have been employed for decades in III–V inorganic semiconductor systems. Understanding and optimizing such inclusions for specific optoelectronic or photovoltaic applications may therefore also become a key target for applications based on future hybrid metal-halide perovskite materials.

In summary, we have investigated the temperature dependent optical absorption and photoluminescence emission from thin $CH_3NH_3PbI_{3-x}Cl_x$-films grown by thermal dual-source evaporation. A broad phase transition exhibiting strong temperature-hysteresis has been located in the range between 100 K and 140 K. During this transition, which we ascribe to the well-established tetragonal-to-orthorhombic phase-transition in the pure triiodide $CH_3NH_3PbI_3$, the absorption edge shifts upwards in photon energy from about 1.6 eV to 1.7 eV. In the room-temperature (tetragonal) phase, the PL emission spectrum consists of a single broad peak in the vicinity of the absorption edge. This peak continues to exist below the phase transition, while a second, smaller peak gradually emerges close to the absorption edge of the low-temperature (orthorhombic) phase. The spectral width of this peak remains constant under further cooling, consistent with polaronic broadening mechanisms as previously proposed to account for the large homogenous emission line width at room temperature. Our observation that, even below the phase transition, PL is dominantly emitted near the bandgap energy of the room-temperature phase may be explained by the presence of small inclusions of the tetragonal crystal structure, in which a large fraction of photoexcited carriers agglomerate. Excitation-energy-dependent PL data show that any possible absorption from such inclusions does at most contribute a negligible amount to carrier generation and therefore indicates that their total volume-fraction in the film is very small. We performed time-resolved PL measurements and observed a clear signature of carrier migration to lower-energy sites. We found very similar lifetimes for higher- and lower-energy

emission indicating that the decay of the photoexcited carrier population is predominantly governed by recombination within the tetragonal crystallites. These lifetimes are, in comparison to those measured above the phase transition, considerably shorter and notably fluence-dependent. This can be explained by the strongly increased carrier density within the inclusions giving rise to significant bi-molecular recombination and hence does not imply intrinsically higher decay rate constants in the orthorhombic phase. Our results demonstrate the potentially strong influence of low-energy sites on the material performance of the organic-inorganic perovskite system even at low volume fraction.

The authors gratefully acknowledge funding from the Engineering and Physical Sciences Research Council.

[1] H.-S. Kim, C.-R. Lee, J.-H. Im, K.-B. Lee, T. Moehl, A. Marchioro, S.-J. Moon, R. Humphry-Baker, J.-H. Yum, J. E. Moser, M. Gratzel, and N.-G. Park, "Lead iodide perovskite sensitized all-solid-state submicron thin film mesoscopic solar cell with efficiency exceeding 9%," Sci. Rep. **2**, 591 (2012).
[2] M. M. Lee, J. Teuscher, T. Miyasaka, T. N. Murakami, and H. J. Snaith, "Efficient hybrid solar cells based on meso-superstructured organometal halide perovskites," Science **338**(6107), 643–647 (2012).
[3] T. C. Sum and N. Mathews, "Advancements in perovskite solar cells: Photophysics behind the photovoltaics," Energy Environ. Sci. **7**, 2518–2534 (2014).
[4] C. C. Stoumpos, C. D. Malliakas and M. G. Kanatzidis, "Semiconducting tin and lead iodide perovskites with organic cations: Phase transitions, high mobilities, and near-infrared photoluminescent properties," Inorg. Chem. **52**(15), 9019–9038 (2013).
[5] C. Wehrenfennig, G. E. Eperon, M. B. Johnston, H. J. Snaith, and L. M. Herz, "High charge carrier mobilities and lifetimes in organolead trihalide perovskites," Adv. Mater. **26**(10), 1584–1589 (2014).
[6] C. S. Ponseca, T. J. Savenije, M. A. Abdellah, K. Zheng, A. P. Yartsev, T. Pascher, T. Harlang, P. Chabera, T. Pullerits, A. Stepanov, J.-P. Wolf, and V. Sundstrom, "Organometal halide perovskite solar cell materials rationalized – Ultrafast charge generation, high and microsecond-long balanced mobilities and slow recombination," J. Am. Chem. Soc. **136**(14), 5189 (2014).
[7] G. Xing, N. Mathews, S. Sun, S. S. Lim, Y. M. Lam, M. Grätzel, S. Mhaisalkar, and T. C. Sum, "Long-range balanced electron- and hole-transport lengths in organic-inorganic $CH_3NH_3PbI_3$," Science **342**(6156), 344–347 (2013).
[8] S. D. Stranks, G. E. Eperon, G. Grancini, C. Menelaou, M. J. P. Alcocer, T. Leijtens, L. M. Herz, A. Petrozza, and H. J. Snaith, "Electron-hole diffusion lengths exceeding 1 micrometer in an organometal trihalide perovskite absorber," Science **342**(6156), 341–344 (2013).
[9] A. Marchioro, J. Teuscher, D. Friedrich, M. Kunst, R. van de Krol, T. Moehl, M. Gratzel, and J.-E. Moser, "Unravelling the mechanism of photoinduced charge transfer processes in lead iodide perovskite solar cells," Nat. Photon. **8**, 250–255 (2014).
[10] S. Sun, T. Salim, N. Mathews, M. Duchamp, C. Boothroyd, G. Xing, T. C. Sum and Y. M. Lam, "The origin of high efficiency in low-temperature solution-processable bilayer organometal halide hybrid solar cells," Energy Environ. Sci. **7**, 339–407 (2014).
[11] V. D'Innocenzo, G. Grancini, M. J. P. Alcocer, A. R. S. Kandada, S. D. Stranks, M. M. Lee, G. Lanzani, H. J. Snaith, and A. Petrozza, "Excitons versus free charges in organo-lead tri-halide perovskites," Nat. Commun. **5**, 3586 (2014).
[12] C. Wehrenfennig, M. Liu, H. J. Snaith, M. B. Johnston, and L. M. Herz, "Homogeneous emission line broadening in the organo lead halide perovskite $CH_3NH_3PbI_{3-x}Cl_x$," J. Phys. Chem. Lett. **5**, 1300–1306 (2014).
[13] J. H. Noh, S. H. Im, J. H. Heo, T. N. Mandal, and S. I. Seok, "Chemical management for colorful, efficient, and stable inorganic–organic hybrid nanostructured solar cells," Nano Lett. **13**(4), 1764–1769 (2013).
[14] G. E. Eperon, S. D. Stranks, C. Menelaou, M. B. Johnston, L. M. Herz, and H. J. Snaith, "Formamidinium lead trihalide: A broadly tunable perovskite for efficient planar heterojunction solar cells," Energy Environ. Sci. **7**, 982–988 (2014).
[15] E. Mosconi, A. Amat, M. K. Nazeeruddin, M. Grätzel and F. De Angelis, "First principles modeling of mixed halide organometal perovskites for photovoltaic applications," J. Phys. Chem. C **117**(27), 13902–13913 (2013).
[16] J. Even, L. Pedesseau, J.-M. Jancu, and C. Katan, "Importance of spin-orbit coupling in hybrid organic/inorganic perovskites for photovoltaic applications," J. Phys. Chem. Lett. **4**(17), 2999–3005 (2013).
[17] S. Colella, E. Mosconi, P. Fedeli, A. Listorti, F. Gazza, F. Orlandi, P. Ferro, T. Besagni, A. Rizzo, G. Calestani, G. Gigli, F. De Angelis, and R. Mosca, "$MAPbI_{3-x}Cl_x$ mixed halide perovskite for hybrid solar cells: The role of chloride as dopant on the transport and structural properties," Chem. Mater. **25**(22), 4613–4618 (2013).
[18] J. Even, L. Pedesseau, J.-M. Jancu, and C. Katan, "DFT and $k \cdot p$ modelling of the phase transitions of lead and tin halide perovskites for photovoltaic cells," Phys. Status Solidi RRL **8**(1), 31–35 (2014).
[19] J. M. Frost, K. T. Butler, F. Brivio, C. H. Hendon, M. van Schilfgaarde, and A. Walsh, "Atomistic origins of high-performance in hybrid halide perovskite solar cells," Nano Lett. **14**, 2584–2590 (2014).
[20] P. Umari, E. Mosconi, and F. De Angelis, "Relativistic GW calculations on $CH_3NH_3PbI_3$ and $CH_3NH_3SnI_3$ perovskites for solar cell applications," Sci. Rep. **4**, 4467 (2014).
[21] Y. Wang, T. Gould, J. F. Dobson, H. Zhang, H. Yang, X. Yao, and H. Zhao, "Density functional theory analysis of structural and electronic properties of orthorhombic perovskite $CH_3NH_3PbI_3$," Phys. Chem. Chem. Phys. **16**, 1424–1429 (2014).
[22] M. Hirasawa, T. Ishihara, T. Goto, K. Uchida, and N. Miura, "Magnetoabsorption of the lowest exciton in perovskite-type compound $(CH_3NH_3)PbI_3$," Physica B **201**(0), 427–430 (1994).
[23] D. Weber, "$CH_3NH_3PbX_3$, ein Pb(II)-system mit kubischer perowskitstruktur," Z. Naturforsch. B **33**, 1443–1445 (1978).

[24] A. Poglitsch and D. Weber, "Dynamic disorder in methylammoniumtrihalogenoplumbates (II) observed by millimeter-wave spectroscopy," J. Chem. Phys. **87**, 6373–6378 (1987).
[25] Y. Kawamura, H. Mashiyama, and K. Hasebe, "Structural study on cubic–Tetragonal transition of $CH_3NH_3PbI_3$," J. Phys. Soc. Jpn. **71**(7), 1694–1697 (2002).
[26] T. Baikie, Y. Fang, J. M. Kadro, M. Schreyer, F. Wei, S. G. Mhaisalkar, M. Graetzel, and T. J. White, "Synthesis and crystal chemistry of the hybrid perovskite $(CH_3NH_3)PbI_3$ for solid-state sensitised solar cell applications," J. Mater. Chem. A **1**, 5628–5641 (2013).
[27] R. Wasylishen, O. Knop, and J. Macdonald, "Cation rotation in methylammonium lead halides," Solid State Commun. **56**(7), 581–582 (1985).
[28] N. Onoda-Yamamuro, T. Matsuo, and H. Suga, "Calorimetric and IR spectroscopic studies of phase transitions in methylammonium trihalogenoplumbates (II)," J. Phys. Chem. Solids **51**(12), 1383–1395 (1990).
[29] N. Onoda-Yamamuro, T. Matsuo, and H. Suga, "Dielectric study of $CH_3NH_3PbX_3$ (X = Cl, Br, I)," J. Phys. Chem. Solids **53**(7), 935–939 (1992).
[30] Y. Yamada, T. Nakamura, M. Endo, A. Wakamiya, and Y. Kanemitsu, "Near-band-edge optical responses of solution-processed organic–inorganic hybrid perovskite $CH_3NH_3PbI_3$ on mesoporous TiO_2 electrodes," Appl. Phys. Exp. **7**(3), 032302 (2014).
[31] M. Liu, M. B. Johnston, and H. J. Snaith, "Efficient planar heterojunction perovskite solar cells by vapour deposition," Nature **501**, 395–398 (2013).
[32] M. D. Sturge, "Optical absorption of gallium arsenide between 0.6 and 2.75 eV," Phys. Rev. **127**, 768–773 (1962).
[33] W. von der Osten and H. Stolz, "Localized exciton states in silver halides," J. Phys. Chem. Solids, **51**(7), 765–791 (1990).
[34] R. Williams and K. Song, "The self-trapped exciton," J. Phys. Chem. Solids **51**(7), 679–716 (1990).
[35] K. Saito, T. Kurosawa, T. Akai, S. Yokoyama, H. Morioka, T. Oikawa, and H. Funakubo, "Characterization of epitaxial $Pb(Zr_x,Ti_{1-x})O_3$ thin films with composition near the morphotropic phase boundary," MRS Proc. **748**, U13.4 (2002).
[36] S. Yokoyama, Y. Honda, H. Morioka, T. Oikawa, H. Funakubo, T. Iijima, H. Matsuda, and K. Saito, "Large piezoelectric response in (111)-oriented epitaxial $Pb(Zr,Ti)O_3$ films consisting of mixed phases with rhombohedral and tetragonal symmetry," Appl. Phys. Lett. **83**(12), 2408–2410 (2003).
[37] M. B. Kelman, P. C. McIntyre, B. C. Hendrix, S. M. Bilodeau, J. F. Roeder, and S. Brennan, "Structural analysis of coexisting tetragonal and rhombohedral phases in polycrystalline $Pb(Zr_{0.35}Ti_{0.65})O_3$ thin films," J. Mater. Res. **18**, 173–179 (2003).
[38] R. J. Zeches, M. D. Rossell, J. X. Zhang, A. J. Hatt, Q. He, C.-H. Yang, A. Kumar, C. H. Wang, A. Melville, C. Adamo, G. Sheng, Y.-H. Chu, J. F. Ihlefeld, R. Erni, C. Ederer, V. Gopalan, L. Q. Chen, D. G. Schlom, N. A. Spaldin, L. W. Martin, and R. Ramesh, "A strain-driven morphotropic phase boundary in $BiFeO_3$," Science **326**(5955), 977–980 (2009).
[39] Z. Chen, L. You, C. Huang, Y. Qi, J. Wang, T. Sritharan, and L. Chen, "Nanoscale domains in strained epitaxial $BiFeO_3$ thin Films on $LaSrAlO_4$ substrate," Appl. Phys. Lett. **96**(25), 252903 (2010).
[40] L. Ehm, L. A. Borkowski, J. B. Parise, S. Ghose, and Z. Chen, "Evidence of tetragonal nanodomains in the high-pressure polymorph of BaTiO3," Appl. Phys. Lett. **98**(2), 021901 (2011).
[41] C. Wehrenfennig, M. Liu, H. J. Snaith, M. B. Johnston, and L. M. Herz, "Charge-carrier dynamics in vapour-deposited films of the organolead halide perovskite $CH_3NH_3PbI_{3-x}Cl_x$," Energy Environ. Sci. **7**, 2269–2275 (2014).
[42] F. Deschler, M. Price, S. Pathak, L. Klintberg, D. D. Jarausch, R. Higler, S. Huettner, T. Leijtens, S. D. Stranks, H. J. Snaith, M. Atature, R. T. Phillips, and R. H. Friend, "High photoluminescence efficiency and optically-pumped lasing in solution-processed mixed halide perovskite semiconductors," J. Phys. Chem. Lett. **5**, 1421–1426 (2014).
[43] G. Xing, N. Mathews, S. S. Lim, N. Yantara, X. Liu, D. Sabba, M. Grätzel, S. Mhaisalkar, and T. C. Sum, "Low-temperature solution-processed wavelength-tunable perovskites for lasing," Nat. Mater. **13**, 476–480 (2014).